

Effect of Ba and rare earths cations on the properties and dehydrocyclization activity of Pt/K-LTL catalysts

Javier M. Grau, Loreto Daza, Xosé L. Seoane and Adolfo Arcoya *

Instituto de Catálisis y Petroleoquímica (CSIC), Campus UAM, Cantoblanco, 28049 Madrid, Spain
E-mail: aarcoya@icp.csic.es

Received 12 November 1997; accepted 25 May 1998

Several Pt/L-zeolite catalysts were prepared by the impregnation method from L-zeolite samples previously exchanged with Ba^{2+} , La^{3+} , Pr^{3+} , Nd^{3+} and Sm^{3+} . Lanthanides (Ln^{3+}) increase the overall dispersion of platinum, measured by $\text{H}_2\text{--O}_2$ titration. TPR and CO/FTIR measurements indicate that these ions modify the distribution of Pt in the zeolite lattice, increasing the fraction of metal on the external surface. Additionally, both CO/FTIR and competitive hydrogenation of toluene–benzene mixtures indicate that, in the presence of Ln^{3+} , the electron density of the platinum decreases in comparison with Pt/KL-zeolite. On the other hand, Ba^{2+} does not substantially modify neither the distribution nor the electronic state of Pt. The reactivity measurements in the hydroconversion of *n*-heptane show that Pt/BaKL and Pt/KL exhibit similar catalytic behaviour with a high dehydrocyclization activity. However, the exchange of K^+ by Ln^{3+} increases the production of heptane isomers, while selectivities to aromatic and terminal hydrogenolysis products significantly decrease.

Keywords: Pt/K-LTL catalysts, barium, rare earths, dehydrocyclization, *n*-heptane, toluene, TPR, CO/FTIR

1. Introduction

Since the high activity and selectivity of the non-acidic Pt/KL-zeolite catalysts in the aromatization of *n*-alkanes was noticed [1] numerous works have been performed to explain the origin of this catalytic behaviour [2–8]. Several authors have reported that aromatization selectivity is very sensitive to the identity of the countercation present in the zeolite, in such a way that for alkaline or alkaline earths cations the bigger the ionic radius the higher the dehydrocyclization activity. Thus, when L-zeolite is exchanged with alkaline ions, the aromatization selectivity of the catalyst for *n*-hexane increases in the order $\text{Li}^+ < \text{K}^+ < \text{Rb}^+ < \text{Cs}^+$ [2,3,9]. In a similar way, Hughes et al. [10] found that alkaline earths increase the aromatization activity in the order $\text{Be}^{2+} < \text{Mg}^{2+} < \text{Ca}^{2+} < \text{Ba}^{2+}$. When comparing the effect of cations with different radius and charge, however, the relationship between basicity and dehydrocyclization activity is not straightforward. Thus, Pt/BaL-zeolite catalysts exhibit similar or higher aromatization activity than Pt/KL-zeolite [10,11], in spite of the fact that the ionic potential of K^+ is lower than the one of Ba^{2+} . In this case, it seems that other effects, in addition to the ionic potential of the charge-compensating cations, can influence the catalytic behaviour. The goal of this research is to analyze the effect of a divalent cation (Ba^{2+}) and several trivalent cations (La^{3+} , Pr^{3+} , Nd^{3+} and Sm^{3+}) on the physicochemical properties of Pt/KL catalysts, as well as on their performances in the conversion of *n*-heptane in presence of hydrogen.

Lanthanides, which display a strong basic character, have shown a remarkable promoter effect of metal catalysts for different reactions [12,13]. However, their effect on Pt/KL catalysts has been scantily investigated [14–16]. As La^{3+} , Pr^{3+} , Nd^{3+} and Sm^{3+} have a very similar ionic radius, the KL-zeolite was exchanged with these cations in order to evaluate the sensitivity of the dehydrocyclization reaction and other properties of the catalysts to the changes of basicity of the zeolite produced by such ions. Catalysts were characterized by $\text{H}_2\text{--O}_2$ titration, TPR and CO/FTIR. Additionally, competitive hydrogenation of toluene and benzene mixtures was used as a chemical method to determine the electronic state of platinum.

2. Experimental

2.1. Catalyst preparation

Fractions of a commercial K-LTL zeolite (Union Carbide SK-45; $\text{K}_9\text{Al}_9\text{Si}_{27}\text{O}_{72}$, in atoms per unit cell) were exchanged with Ba^{2+} , La^{3+} , Pr^{3+} , Nd^{3+} and Sm^{3+} . 300 ml of aqueous solutions of nitrates containing 215 meq of these cations ($\text{Me}^{n+}/\text{K}^+ = 2/1$ eq/eq), were added dropwise to a suspension of 30 g of zeolite in 500 ml of distilled water under stirring. After 72 h at reflux temperature, the slurry was filtered and washed with distilled water to remove occluded ions and then dried at 393 K and calcined at 873 K for 6 h. The powder was pelleted and crushed to 0.6–1 mm particle size and then platinum was incorporated by incipient wetness impregnation, using $\text{Pt}(\text{NH}_3)_4(\text{OH})_2$ aqueous solutions in adequate concentration to obtain 1 wt% of Pt

* To whom correspondence should be addressed.

Table 1
Catalysts characterization.

Catalyst	Counter. content ^a (meq/u.c.)		IE (%)	Pt _t (wt%)	D (%)
	K ⁺	Me ⁿ⁺ ^b			
Pt/KL	9.0	0.0	–	0.95	42
Pt/KBaL	6.6	2.4	26.9	0.96	40
Pt/KLaL	6.8	2.2	24.1	0.93	61
Pt/KPrL	6.6	2.4	26.6	0.97	71
Pt/KNdL	7.0	2.0	21.6	1.04	69
Pt/KSmL	7.2	1.8	20.4	0.94	66

^a Based on O = 72.

^b Meⁿ⁺ = Ba²⁺, La³⁺, Pr³⁺, Nd³⁺ or Sm³⁺.

in the catalysts. After drying, the solids were successively calcined under O₂ stream at 573 K for 3 h and reduced with H₂ at 773 K for 3 h. In both cases, the temperature was ramped at 2 K/min. The reduced catalysts were stored in a desiccator. Their chemical composition, given in table 1, was determined by atomic absorption spectroscopy (AAS).

2.2. Catalyst characterization

2.2.1. Chemisorption measurements

Platinum dispersion (*D*) in the reduced catalyst is defined as $D = Pt_s/Pt_t$, where Pt_s is the number of metal atoms exposed per gram of catalyst and Pt_t is the total number of metal atoms loaded in 1 g of catalyst. Pt_s was obtained by the H₂–O₂ titration method [17] in a flow system with a thermal conductivity detector. Samples of 0.5 g of reduced catalysts were heated at 723 K under H₂ stream for 30 min. After evacuation under a flow of Ar for 1 h at 573 K and cooling at room temperature, pulses of O₂ were introduced in the carrier gas until total saturation of the metal surface. Titration of the adsorbed O₂ was performed with H₂ at room temperature. From the volume of hydrogen uptake and assuming an atomic stoichiometry $H_{up}/Pt_s = 3/1$, the number of exposed Pt atoms was calculated. Pt_t was obtained by AAS analysis.

2.2.2. Temperature-programmed reduction

TPR profiles of the calcined precursors were obtained in a flow system with a thermal conductivity detector. Samples of 0.5 g were outgassed at 573 K for 1 h under an argon stream. After cooling, the profiles were registered heating the samples from 273 to 813 K at 8 K min^{−1} under a flow of 60 cm³ min^{−1} of a mixture of 5% H₂/Ar.

2.2.3. Infrared spectroscopy

FTIR spectra of the reduced catalysts were recorded at room temperature in a Nicolet 5ZDX spectrometer, in the range 4800–400 cm^{−1} with a resolution of 4 cm^{−1}. The self-supported wafer of the reduced sample was successively outgassed at 10^{−2} Pa and 723 K for 1 h, treated at 723 K under hydrogen atmosphere for 2 h and outgassed at 10^{−2} Pa for 2 h at 298 K. After recording the IR spectra, the samples were contacted with 4 kPa of CO for 5 min

and then a new spectrum was recorded. The bands of the chemisorbed CO were obtained by subtraction of both spectra. In order to gain information about the location of Pt clusters in the zeolite lattice, a new spectrum of CO was taken after outgassing at 523 K for 30 min.

2.3. Reactivity measurements

The catalytic activity measurements in the dehydrocyclization of *n*-heptane were performed in a fixed-bed tubular reactor, containing 2 g of catalyst, diluted with SiC, at 100 kPa, 723 K, H₂/*n*-C₇ = 7.3 mol/mol and a liquid space velocity of 3.42 h^{−1}. A bed of SiC above the catalyst was employed as preheater. High-purity hydrogen was successively passed through a Deoxo purifier and a 5A molecular sieve filter. The reactor was heated at 773 K for 1 h under the adequate hydrogen flow and, when the reaction temperature was stabilized at 723 K, the liquid feed was introduced and the first sample collected 15 min later. Following a conventional methodology [18,19], we had previously confirmed that in these experimental conditions both external and internal diffusion limitations were absent.

The reactor effluent was condensed at 273 K and analyzed by gas–liquid chromatography (TCD). Liquid samples were injected in a 4 m × 3.18 mm O.D. column packed with 1,2,3-tris(2-cyanoethoxy)propane (10 wt%) on Chromosorb P (60–80 mesh) at 353 K. The exit gas stream was analyzed at 313 K in a 4 m × 3.18 mm O.D. column of powdered activated charcoal. Helium (40 cm³ min^{−1}) was used as carrier gas.

Competitive hydrogenation of toluene/benzene mixtures was carried out in a conventional flow reactor with 0.5 g of catalyst at 373 K and atmospheric pressure. The benzene and hydrogen pressures did remain constant, while that of toluene was modified in the range 1.9–9.6 kPa. The total flow was 125 cm³ min^{−1} (STP) and the conversion was always lower than 10%. Prior to the reaction, the catalyst was treated at 723 K under flow of hydrogen for 30 min. Reaction products were analyzed on line in a FID chromatograph at 373 K with a 20% CW 20 M on supercoport 80/100 packed column. Helium (20 cm³ min^{−1}) was used as carrier gas.

3. Results and discussion

3.1. Catalyst characterization

Table 1 summarizes the cations content per u.c. and the degree of exchange reached for each zeolite support. The degree of exchange (*IE*) is defined as the number of equivalents of a cation exchanged per 100 equivalents of K⁺. Platinum loaded (Pt_t) and metal dispersion (*D*%) for the catalysts are also included. The degree of exchange reached is very much the same for all the samples. The dispersion values found for Pt/KL and Pt/KBaL are very similar (about 40%), while with the incorporation of the rare earths it went up to 60–70%.

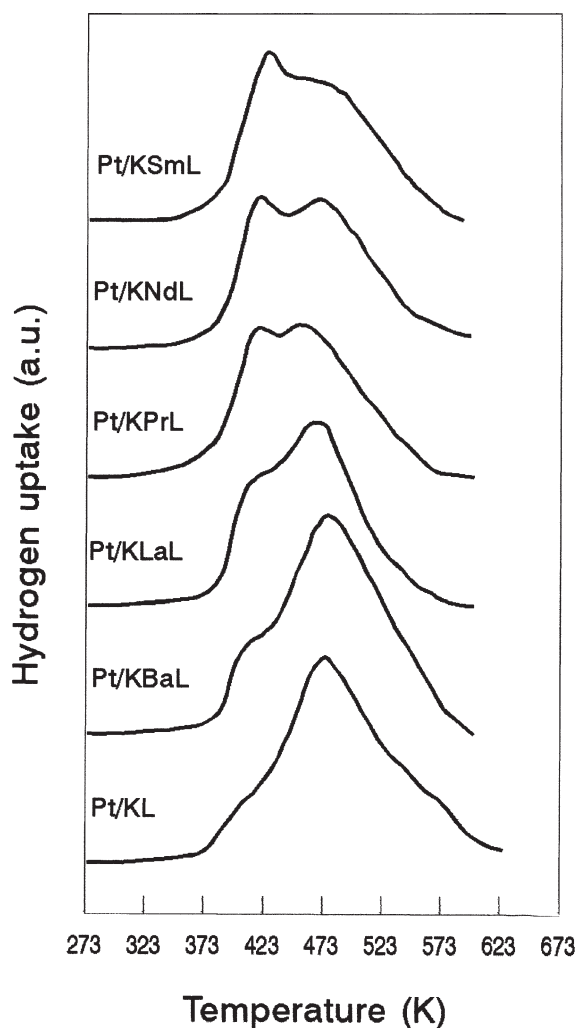


Figure 1. TPR profiles of the catalysts.

3.1.1. TPR measurements

The TPR profiles of the catalyst precursors (figure 1) show that complete reduction of Pt occurs below 623 K, indicating that in the conditions used to prepare the catalysts they are completely reduced. The profile of Pt/KL shows a broad reduction peak at 475 K with a shoulder at 408 K. This profile substantially agrees with that obtained by Osgard et al. [20] for a 0.5% Pt/KL-zeolite prepared by impregnation using $\text{Pt}(\text{NH}_3)_4\text{Cl}_2$ as precursor. In our case, however, the TPR maximum appears at a lower temperature (about 48 K), probably due to the different nature of the precursors used: $\text{Pt}(\text{NH}_3)_4(\text{OH})_2$. The same authors [20] reported that the Pt/KL catalysts prepared by impregnation contain, after calcination, predominantly Pt^{4+} ions within the zeolite channels, originated by autoreduction of Pt^{2+} and their subsequent oxidation to PtO_2 . Although this reaction is feasible, we think that in our catalyst, after calcination, most of platinum is located inside the pores as Pt^{2+} . This suggestion is supported by the fact that the ratio H_2 uptake/ P_t is about 1.35, which corresponds to 65% Pt^{2+} and 35% Pt^{4+} . In such a case, one can expect that the broad peak

Table 2
Physical parameters of the cations.

Cation	Ionic radius (\AA)	ϕ^a
K^+	1.33	0.75
Ba^{2+}	1.35	1.48
La^{3+}	1.15	2.60
Pr^{3+}	1.09	2.75
Nd^{3+}	1.08	2.77
Sm^{3+}	1.04	2.88

^a ϕ = ionic potential of the cations = ionic charge/ionic radius.

at 475 K includes the reduction of both PtO and PtO_2 species, in order to account for the average platinum valence observed. The shoulder at 408 K, on the other hand, must be related to a platinum species more easily reducible than the preceding one, probably Pt^{2+} located on the external surface of the zeolite, i.e., on the intercrystalline space.

As shown in figure 1, the incorporation of Ba^{2+} or Ln^{3+} (lanthanides) to the zeolite substantially modifies the TPR profile of Pt/KL. The relative intensity of the peak at 475 K decreases, whereas the shoulder at 408 K shifts to higher temperatures and its intensity increases with the increase of the ionic potential of the compensating cation, i.e., ϕ = ionic charge/ionic radius ($\text{K}^+ < \text{Ba}^{2+} < \text{La}^{3+} < \text{Pr}^{3+} < \text{Nd}^{3+} < \text{Sm}^{3+}$, table 2). For the Pt/KPrL sample, the intensity of both peaks is similar, while for the Pt/KSmL catalyst, the second peak is the most important one and appears at 426 K. These results suggest that the change of the ionic potential of the counteranions affects not only the relative population of the different forms of platinum, but also the strength of the platinum-zeolite interaction of the more easily reducible Pt form.

3.1.2. Infrared spectroscopy

The FTIR spectra of the adsorbed CO on the catalysts are depicted in figure 2. All the spectra exhibit a broad band in the range $2150\text{--}1925\text{ cm}^{-1}$, with a maximum at 2073 cm^{-1} and several shoulders, which are assigned to CO linearly bonded to Pt species supported on LTL [2,3,21]. Bands below 1900 cm^{-1} , attributed to bridged carbonyls on Pt, are very weak and they were not included in figure 2.

For non-zeolitic supports, the frequency of the maximum at ca. 2073 cm^{-1} corresponds to CO chemisorbed on non-interacting metal [22–24]. With regard to Pt/KL catalysts, this signal is also associated to CO bonded to non-interacting platinum particles, located in the outer surface of the zeolite [2,3,21]. On the other hand, the shoulders at 2053 and 2012 cm^{-1} are ascribed to Pt clusters inside the zeolite, but in different environments [9,21]. Finally, the band appearing at 2120 cm^{-1} is taken as evidence for the existence of electron-deficient platinum sites [2,24–26].

When comparing the IR spectra in figure 2, it is observed that the intensity of the shoulder at ca. 2120 cm^{-1} grows and the peak at 2073 cm^{-1} shifts to 2080 cm^{-1} with increasing ionic potential of the cation ($\text{Pt/KL} <$

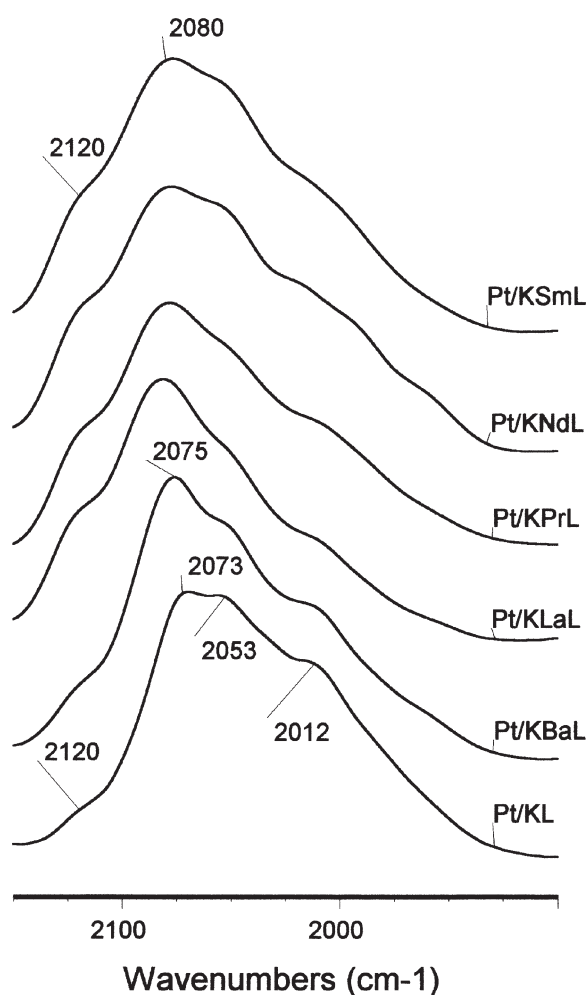


Figure 2. FTIR spectra of CO adsorbed on the catalysts at room temperature and 4 kPa.

Pt/KBaL \ll Pt/KLaL \leq Pt/KPrL \leq Pt/KNdL \leq Pt/KSmL). These results indicate that the relative abundance of the electron-deficient platinum species ($\text{Pt}^{\delta+}$) increases with the ionic potential of the charge-compensating cations.

Since CO bonded to the Pt cluster located on the external surface of the zeolite is easily removable [21], additional information can be deduced from the feature of the IR spectra obtained after outgassing at 523 K the chemisorbed CO (figure 3). The shift of the wavenumber of the band at 1962 cm^{-1} to 1983 cm^{-1} in the order Pt/KL < Pt/KBaL < Pt/KLaL < Pt/KPrL < Pt/KNdL < Pt/KSmL, together with the increase of the intensity of the band at 2032 cm^{-1} in the same sequence, indicate a parallel decrease of the electron density of Pt inside the channels [25]. Probably, the stronger interaction of the Ln^{3+} cations with the oxygens of the walls of the framework [27] causes the electron density decrease observed for Pt clusters in these catalysts. However, an alternative explanation, based on the direct interaction Pt-counteranion in the way described by Stakheev et al. [21] for Pt/K(Me)L catalysts, may also be plausible. The fact that no bands are detected in the spectra of figure 3 at wavenumbers higher than 2080 cm^{-1} sug-

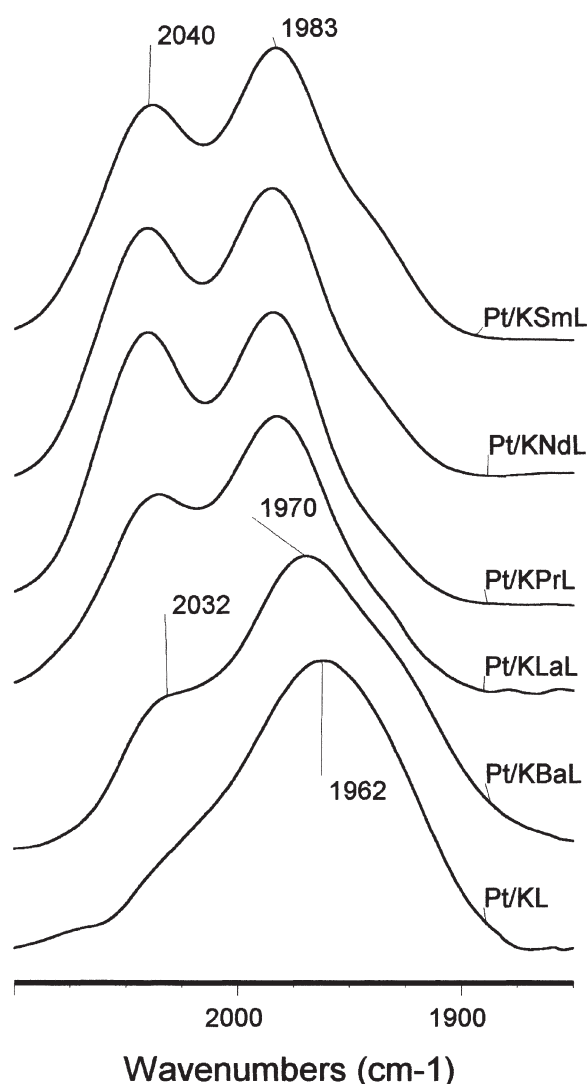


Figure 3. FTIR spectra of CO remaining on the catalysts upon adsorption at room temperature and 4 kPa and subsequent evacuation at 523 K and 10^{-2} Pa .

gests that electron-deficient Pt species (band at 2120 cm^{-1} in figure 2) can be located on the external surface of the zeolite.

3.2. Reactivity of the catalysts

Table 3 shows the performances of the catalysts in the conversion of *n*-heptane at 723 K, after 15 min on stream. The reaction leads to aromatics (toluene and benzene), heptane isomers (*i*-C₇), methane, hydrocracking products (C₂–C₆) and cycloalkanes. Conversion of *n*-heptane is defined as the number of molecules of *n*-heptane transformed per 100 molecules fed to the reactor and the yield to toluene (Y_{Tol}) is calculated as the number of molecules of *n*-heptane transformed into toluene per 100 molecules of *n*-heptane fed. The selectivity to a product *i* (S_i) is defined as the number of *n*-heptane molecules transformed into *i* per 100 molecules of *n*-heptane converted. The turnover frequency

Table 3
Reactivity of the catalysts in *n*-heptane conversion and $K_{T/B}$ values.

	Catalyst					
	Pt/KL	Pt/KBaL	Pt/KLaL	Pt/KPrL	Pt/KNdL	Pt/KSmKL
Conversion (%)	21.2	20.7	12.7	11.3	9.6	9.2
TOF $\times 10^3$ (s ⁻¹)	92.9	95.2	38.3	29.3	25.6	25.7
Y_{Tol}	9.1	8.9	2.4	2.3	1.9	1.7
TOF _{Tol} $\times 10^3$ (s ⁻¹)	39.9	40.9	7.2	5.9	5.1	4.7
Selectivity (mol%)						
Toluene	42.9	43.0	18.9	20.3	20.0	18.5
Benzene	5.2	7.6	0.0	0.0	0.0	0.0
Methane	5.6	7.2	2.4	0.8	1.0	0.0
C ₂ –C ₆	17.4	17.3	25.9	25.0	24.0	27.0
<i>i</i> -heptane	15.7	12.5	48.0	50.4	51.0	49.1
Cycloalkanes	13.2	12.0	4.7	3.5	4.1	5.4
$K_{T/B}$	1.9	2.0	3.6	3.7	3.8	3.8

(TOF) is the number of *n*-heptane molecules transformed per exposed platinum atom per second.

Data in table 3 show that Pt/KL and Pt/KBaL are the most active catalysts for *n*-heptane conversion, in spite of the fact that they have lower number of exposed platinum atoms than the samples containing lanthanides (table 1). On the other hand, Pt/KL and Pt/KBaL give a similar product distribution, aromatization being the most favoured reaction ($S_{Tol} = 42.9\%$), while for lanthanide-containing catalysts hydroisomerization of *n*-heptane is the main reaction ($S_{i\text{-heptane}} = 48\text{--}51\%$). Since the ionic potentials of lanthanides cations are higher than those of Ba²⁺ or K⁺ (table 2), these results agree with the general idea that a basic environment of Pt is essential to transform *n*-paraffins into aromatic. Thus, if one assumes that all the Pt_s atoms measured by H₂–O₂ titration are active for *n*-heptane dehydrocyclization, the lower the ionic potential of the counteranion the higher TOF of aromatization.

The ionic potential (ϕ) is a measure of the electron acceptor–donor capacity of the cation (i.e., its polarizing power) in its close vicinity. Therefore, ϕ is an important physicochemical parameter of the counteranion to explain the relative electronic state of the metal in a series of catalysts and, consequently, their activity and selectivity in the reaction under study. The ionic potential, however, does not seem to be the only property to be taken into account in order to rationalize the behaviour of these catalytic systems. In fact, the location and mobility of the incorporated cation inside the zeolite channels can also modify the state of platinum. For this reason, in order to know the actual electronic properties of platinum, it is necessary to measure them directly on each catalyst. To do this, we have used the competitive hydrogenation of toluene–benzene mixtures. This is a structure-insensitive reaction, but the ratio of the adsorption coefficients of toluene and benzene ($K_{T/B}$) is a very sensitive thermodynamic function of the electronic state of the Pt particles in the catalyst. The $K_{T/B}$ values were obtained from the rela-

tive hydrogenation rates of toluene and benzene, following the method of Tri et al. [28], which was used by Larsen and Haller [29] to estimate the chemical state of Pt supported on L-zeolite. Since the ionization energy of toluene (8.82 eV) is lower than that of benzene (9.25 eV) [30] (i.e., toluene is a better electron donor than benzene), it will be preferentially adsorbed on the more electrophilic metal sites, thus hindering the adsorption of benzene. Consequently, the higher the electron density of the metal the lower the $K_{T/B}$.

The order of increase of $K_{T/B}$ values, summarized in table 3, is parallel to both the increase of the IR band intensity at ca. 2120 cm⁻¹, related to the electron-deficient platinum (figure 2), and the positive shift of the IR bands of the irreversibly adsorbed CO (figure 3). On the other hand, a relationship between $K_{T/B}$ and the toluene turnover frequency (TOF_{Tol} in table 3) is also evident, in agreement to what one should expect. These findings indicate that an effect of the counteranions on the platinum atoms exists, probably through the oxygen of the zeolite framework, as it was suggested by Barthomeuf [27]. The fact that the $K_{T/B}$ values and the catalytic properties of Pt/KL and Pt/KBaL are very similar is not surprising, in spite of the fact that the ionic potential of Ba²⁺ and, consequently, its Lewis acid character is higher than that of K⁺. It was reported [10,31] that, after the exchange step, the Ba²⁺ cations are located at the open sites of the zeolite, where the reaction



can take place, generating Brønsted acid sites. However, by thermal treatment the Ba²⁺ ions move to sites inaccessible to water molecules, preventing the Ba²⁺ hydrolysis reaction [27]. In such a case, the electronic state of Pt depends, to a great extent, on the mobility and definitive location of the cations in the lattice, in such a way that the dehydrocyclization activity of a catalyst can be different to that expected from ϕ values.

For lanthanides-containing catalysts, a parallel trend is observed between both Y_{Tol} and TOF_{Tol} values and ϕ or $K_{\text{T/B}}$. The differences between the dehydrocyclization activity of these samples reasonably agree with the ionic potential, but they are relatively higher than those expected from the $K_{\text{T/B}}$ values, which are experimental measurements of the basicity of the platinum ensembles. Therefore, these results suggest that the dehydrocyclization is sensitive to the slight changes in the platinum basicity originated by the lanthanide cations.

It is interesting to point out that the selectivity of aromatization correlates to the terminal hydrogenolysis selectivity of the catalysts, as also found by Iglesia and Baumgartner [5] for dehydrocyclization of *n*-heptane on Pt/KL catalysts. Since hydrogenolysis requires metal ensembles with an electron donor character, the practical disappearance of methane on catalysts containing lanthanides can be related to the reduction of the electron density of the metal in these catalysts, due to the relatively high Lewis acidity of those cations. Such electronic changes could explain why benzene is not formed on these catalysts which, in fact, behave rather as hydroconversion bifunctional catalysts.

4. Conclusions

The surface properties and the dehydrocyclization activity and selectivity of Pt/KL-type catalysts depend on the identity of the countercations in the zeolite. The partial exchange of K^+ by Ba^{2+} does not substantially modify the dispersion, nor TPR and CO/FTIR spectra, nor *n*-heptane aromatization activity of the Pt/KL catalyst. These results agree with the similar platinum basicity exhibited by the Pt/KL and Pt/KBaL catalysts, as measured from the $K_{\text{T/B}}$ values, in spite of the fact that Ba^{2+} is a stronger Lewis acid than K^+ . This behaviour is probably related to the capability of the Ba^{2+} cation to emigrate upon thermal treatment to zeolite sites where the hydrolysis of the water is not possible.

When K^+ is exchanged with La^{3+} , Pr^{3+} , Nd^{3+} or Sm^{3+} , the dehydrocyclization and hydrogenolysis activities of the catalysts are lower and their isomerization activity higher than for both Pt/KL and Pt/KBaL. This behaviour is probably a consequence of the increase of the amount of electron-deficient platinum in Pt/KLnL samples, as evidenced by FTIR and in agreement with the values of $K_{\text{T/B}}$. On the other hand, the differences of aromatization activity between Pt/La-, Pr-, Nd- and Sm-KL catalysts are small, as expected from the close similarity between the physico-chemical properties of the lanthanides ions. These differences, however, are higher than those between the corresponding values of $K_{\text{T/B}}$.

Acknowledgement

Financial support from CICYT (Project MAT95/0789) is gratefully acknowledged. JMG is also grateful for a CONICET (Argentina) fellowship.

References

- [1] J.R. Bernard, in: *Proc. 5th Int. Conf. Zeolites*, ed. L.W. Rees (Heyden, London, 1980) p. 686.
- [2] C. Besoukhanova, J. Guidot, D. Barthomeuf, M. Breyse and J.R. Bernard, *J. Chem. Soc. Faraday Trans. I* 77 (1981) 1595.
- [3] W. Han, A.B. Kooh and R.F. Hicks, *Catal. Lett.* 18 (1993) 193.
- [4] S.J. Tauster and J.J. Steger, *J. Catal.* 125 (1990) 387.
- [5] E. Iglesia and J.E. Baumgartner, *Stud. Surf. Sci. Catal.* 75 (1993) 993.
- [6] W.H. Han, A.B. Kooh and R.F. Hicks, *Catal. Lett.* 18 (1993) 219.
- [7] S.B. Sharma, J.T. Miller and J.A. Dumesic, *J. Catal.* 148 (1994) 198.
- [8] E. Mielczarski, S.B. Hong, R.J. Davis and M.E. Davis, *J. Catal.* 134 (1992) 349.
- [9] R.F. Hicks, W.J. Han and A.B. Kooh, *Stud. Surf. Sci. Catal.* 75 (1993) 1043.
- [10] T.R. Hughes, W.C. Buss, P.W. Tamm and R.L. Jacobson, *Stud. Surf. Sci. Catal.* 28 (1986) 725.
- [11] E.G. Derouane and D.J. Vanderveken, *Appl. Catal.* 45 (1988) L15.
- [12] N.Yu. Nogin, N.V. Chesnokov and V.I. Kovalchuk, *Catal. Lett.* 23 (1994) 79.
- [13] A.L. Borer and R. Prins, *J. Catal.* 144 (1993) 439.
- [14] S. Sivasanker, S.G. Hegde, S.V. Awate, S.R. Padalkar and S.B. Kulkarni, *React. Kinet. Catal. Lett.* 36 (1988) 173.
- [15] X. Fang, F. Li and L. Luo, *Appl. Catal. A* 146 (1996) 297.
- [16] P.N. Joshi, R. Bandyopadhyay, S.V. Awate, V.P. Shiralkar and B.S. Rao, *React. Kinet. Catal. Lett.* 53 (1994) 231.
- [17] L. Benson and M. Boudart, *J. Catal.* 4 (1965) 704.
- [18] O. Levenspiel, *Chemical Reaction Engineering* (Wiley, New York, 1966) chapter 14.
- [19] N.S. Fígoli, P.C. L'Argentiere, A. Arcoya and X.L. Seoane, *J. Catal.* 155 (1995) 95.
- [20] D.J. Osgard, L. Kustov, K.R. Poeppelmeier and W.M.H. Sachtler, *J. Catal.* 133 (1992) 342.
- [21] A.Y. Stakheev, E.S. Shpiro, E.I. Jaeger and G.S. Schulz-Ekloff, *Catal. Lett.* 32 (1995) 147.
- [22] F. Pinna, M. Selva, M. Signoreto, G. Strukul, F. Boccuzzi, A. Benedetti, P. Canton and G. Fagherazzi, *J. Catal.* 150 (1994) 356.
- [23] P. Marécot, A. Akhachane and J. Barbier, *Catal. Lett.* 36 (1996) 37.
- [24] W. Juszyk, Z. Karpinski, I. Ratajczykowa, Z. Stanasiuk, J. Zielinski, L.L. Sheu and W.M.H. Sachtler, *J. Catal.* 120 (1989) 68.
- [25] L.M. Kustov, D. Ostgard and W.M.H. Sachtler, *Catal. Lett.* 9 (1991) 121.
- [26] X.L. Seoane, N.S. Fígoli, P.C. L'Argentiere, J.A. González and A. Arcoya, *Catal. Lett.* 47 (1997) 213.
- [27] D. Barthomeuf, *Catal. Rev. Sci. Eng.* 38 (1996) 521.
- [28] R.M. Tri, J. Massadier, P. Galezot and B. Imelik, *Stud. Surf. Sci. Catal.* 11 (1982) 14.
- [29] G. Larsen and G.L. Haller, *Catal. Lett.* 3 (1989) 403.
- [30] E.K. Rideal, *Concepts in Catalysts* (Academic Press, London, 1968) chapter 7.
- [31] G. Larsen and G.L. Haller, *Catal. Lett.* 17 (1993) 127.